MECHANICAL BEHAVIOR AND FAILURE OF SANDWICH STRUCTURES

E.E. GDOUTOS
School of Engineering, Democritus University of Thrace
GR-671 00 Xanthi, Greece. E-mail: egdoutos@civil.duth.gr

The failure behavior of composite sandwich beams under three- and four-point bending was studied. The beams were made of unidirectional carbon/epoxy facings and various core materials including PVC closed-cell foams, a polyurethane foam and an aluminum honeycomb. Various failure modes including facing wrinkling, indentation failure and core failure were observed and compared with analytical predictions. It was established that the initiation, propagation and interaction of failure modes depend on the type of loading, constituent material properties and geometrical dimensions. 11 Ref., 2 Tables, 4 Figures.

Keywords: *investigation of failure behavior, three-point bending, sandwich beams, carbon-epoxy facing, various core materials, strength-to-weight ratio*

Sandwich structures consisting of strong and stiff facings and light weight cores offer improved stiffness and strength to weight ratios compared to monolithic materials. Under flexural loading the facings carry almost all of the bending, while the core takes the shear loading and helps to stabilize the facings. Facing materials include metals and fiber reinforced composites. The latter are being used in advanced applications due to the large strength-to-weight ratio. The core materials mainly include honeycombs, foams and wood.

Possible failure modes of sandwich structures include tensile or compressive failure of the facings, debonding at the core/facing interface, indentation failure under concentrated loads, shear core failure, wrinkling of the compression face and global buckling. Recently, the authors have performed a thorough investigation of the failure behavior of sandwich beams with facings made of carbon/epoxy composite material and core made of foam materials [1–6].

In the present work, failure modes were investigated experimentally in sandwich beams under four-point and three-point bending. Failure modes observed and studied include core failure, face sheet wrinkling and indentation failure.

Materials and specimens. The sandwich beams were fabricated from 8-ply unidirectional carbon/epoxy (AS4/3501-6) facings and various core materials. The facings were bonded to the core with an epoxy adhesive (Hysol EA 9430). The assembly was cured at room temperature. The facings and core had a thickness of 1

Table 1. Properties of balsa wood, aluminum and foam-filled honeycomb, and polyurethane materials

Property	Balsa Wood CK57	Aluminum Honeycomb PAMG 5052	Foam Filled Honeycomb Style 20	Polyurethane FR-3708
Density, ρ, kg/m^3 (lb/ft^3)	150 (9.4)	130 (8.1)	128.3 (8)	128.3 (8)
In-plane long. comp. elast. mod., E_{1c}, MPa (ksi)	129.5 (18.8)	9.5 (1.38)	24.1 (3.5)	38.5 (5.6)
In-plane long. tens. elast. mod., E_{1t}, MPa (ksi)	93.6 (13.6)	4.5 (0.65)	1.3 (0.19)	416.6 (60.4)
In-plane trans. comp. elast. mod., E_{2c}, MPa (ksi)	129.5 (18.7)	6 (0.87)	7.6 (1.1)	38.5 (5.6)
Out of plane comp. elast. mod., E_{3c}, MPa (ksi)	5394 (782.3)	2125 (308)	269.1 (39)	108.7 (15.8)
Transverse shear elast. mod., G_{13}, MPa (ksi)	58.7 (8.5)	579 (84)	8.5 (1.23)	10.3 (1.49)
In-plane long. comp. strength, F_{1c}, MPa (ksi)	0.78 (0.11)	0.2 (0.03)	0.4 (0.06)	1.15 (0.17)
In-plane long. tensile strength, F_{1t}, MPa (ksi)	1.13 (0.16)	1.63 (0.24)	0.48 (0.07)	1.1 (0.16)
In-plane trans. comp. strength, F_{2c}, MPa (ksi)	0.78 (0.11)	0.17 (0.03)	0.32 (0.05)	1.15 (0.17)
Out of plane comp. strength, F_{3c}, MPa (ksi)	9.6 (1.39)	11.8 (1.7)	1.35 (0.2)	1.74 (0.25)
Transverse shear strength, F_{13}, MPa (ksi)	3.75 (0.54)	3.45 (0.5)	0.75 (0.11)	1.4 (0.2)

Table 2. Properties of carbon/epoxy facings, adhesive, and H100 and H250 PVC foams

	Facing	FM-73 adhesive	Foam Core (H100)	Foam Core (H250)
Density, ρ, kg/m^3	1.620	1.180	100	250
Thickness, h, mm	1.01	0.05	25.4	25.4
Longitudinal modulus, E_1, MPa	147.000	1.700	120	228
Transverse modulus, E_3, MPa	10.350		139	403
Transverse shear modulus, G_{13}, MPa	7.600	110	48	117
Longitudinalcompressive strength, F_{1c}, MPa	1.930		1.7	4.5
Transverse compressive strength, F_{3c}, MPa	240		1.9	6.3
Transverse shear strength, F_{13}, MPa	71	33	1.6	5.0

and 25.4 mm, respectively. Beam specimens 25.4 mm wide and of various lengths were cut from the sandwich plates. Tables 1 and 2 give some characteristic properties of the sandwich constituent materials.

Experimental procedure. Special test fixtures were fabricated to provide three- and four-point bending for beams of various lengths. Five span lengths of 10.2, 20.3, 25.4, 40.6 and 76.2 cm were tested. In studying the effects of pure bending, special reinforcement was provided for the core at the outer sections of the beam to prevent premature core failures. Also, under three-point bending, the faces directly under concentrated loads were reinforced with additional layers of carbon/epoxy to suppress and prevent indentation failure. Only in the case when the indentation failure mode was studied, there was no face reinforcement. The concentrated load was applied to the specimens with a cylinder of diameter of 25.4 mm (1 in.).

Strains on the outer and inner (interface between facing and core) surfaces of the facings were recorded with strain gages. Most gages were oriented along the axis of the beam, but some were mounted in the transverse direction to record transverse strains. Beam deflections were measured with a displacement transducer (LVDT) and by monitoring the crosshead motion. The deflection was also monitored with a course moire grating (31 lines/cm). Longitudinal and transverse strains in the core were measured with finer moire gratings of 118 and 200 lines/cm. The deformation of the core was also monitored with birefringent coatings using reflection photoelasticity.

Failure modes. A number of failure modes were recorded and studied in the composite sandwich beams subjected to three- and four-point bending. They include wrinkling of the compression facing, core failure and indentation of the loaded face. These failure modes are discussed in the following sections.

Compression facing wrinkling. Compression facing wrinkling failures were observed in sandwich beams under both four-point and three-point bending. Figure 1 shows moment versus strain results for two different tests of sandwich beams with Divinycell H100 cores under four-point bending. Evidence of wrinkling is shown by the sharp change in recorded strain on the compression facing, indicating inward and outward wrinkling in the two tests. In both cases the critical wrinkling stress was σ_{cr} = 673 MPa.

Wrinkling is a localized short-wave buckling of the compression facing. Wrinkling may be viewed as buckling of the compression facing supported by an elastic continuum, the core. The critical wrinkling stress according to Heath [7] is given by

$$\sigma_{cr} = \left[\frac{2}{3}\frac{h_f}{h_c}\frac{E_{c3}E_{f1}}{(1-\nu_{12}\nu_{21})}\right]^{12}, \quad (1)$$

where h_f, h_c — facing and core thicknesses, respectively; E_{f1}, E_{c3} — facing and core moduli, respectively; ν_{ij} — Poisson's ratio associated with loading in the i-direction and strain in the j-directio; and the indices 1 and 3 refer to the in-plane and through-the-thickness directions, respectively.

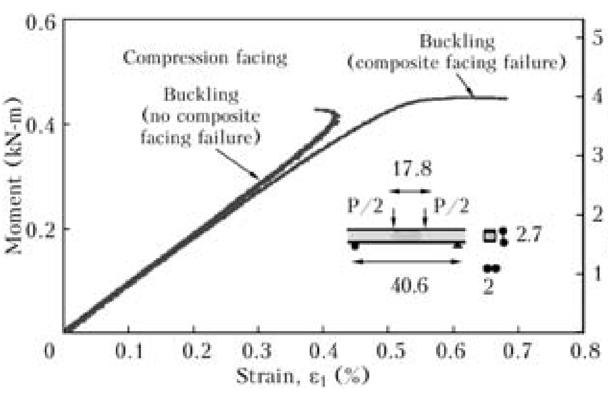

Figure 1. Facing wrinkling in sandwich beam under four-point bending (Divinycell H100 foam core; dimensions are in cm)

Equation (1) predicts the following value of the wrinkling stress σ_{cr} = 687 MPa.

This value is close to the experimental value of 673 MPa.

In the case when shear is present in addition to bending, the influence of the transverse shear modulus of the core, G_{c13}, must be taken into account. An expression given by Hoff and Mautner [8] has the form

$$\sigma_{cr} = c(E_{f1}E_{c3}G_{c13})^{1/3}, \qquad (2)$$

where c is a constant usually taken as equal to 0.5, 0.6, or 0.65. Note that the critical stress in this expression depends only on the elastic moduli of the facing and core materials. In the relation above the core moduli are the initial elastic moduli if wrinkling occurs while the core is still in the linear elastic range. This requires that the shear force at the time of wrinkling be low enough or, at least,

$$V < A_c F_{cs}, \qquad (3)$$

where A_c is core cross sectional area and F_{cs} the shear strength of the core. This is the case for long span beams under three-point bending.

Core failure. Core failures were observed in sandwich beams under three-point bending. The core carries primarily the applied shear loading. In short beams under three-point bending the core is mainly subjected to shear and failure occurs when the maximum shear stress reaches the critical value (shear strength) of the core material. In long-span beams the normal stresses in the core become of the same order of magnitude or even higher than the shear stresses. In this case, the core is subjected to a biaxial state of stress and fails according to an appropriate failure criterion. It was shown that failure of the core materials can be described by the Tsai-Wu failure criterion [9]. For a beam loaded under combined bending and shear, the foam is subjected to longitudinal normal stress, σ_1, and in-plane shear stress, τ_5 (τ_{13}). The Tsai-Wu criterion for this case takes the form

$$f_1\sigma_1 + f_{11}\sigma_1^2 = 1 - k^2, \qquad (4)$$

where

$$f_1 = \frac{1}{F_{1t}} - \frac{1}{F_{1c}}, \quad f_{11} = \frac{1}{F_{1t}F_{1c}}, \quad f_{55} = \frac{1}{F_5^2}, \quad k = \frac{\tau_5}{F_5},$$

F_{1t}, F_{1c} = tensile and compressive strengths in the in-plane (1, 2) direction. F_5 = shear strength on the 1–3 plane.

In the above equations σ_1, σ_3 and τ_5 are the normal and shear stresses referred to the principal material directions (in-plane is direction 1 and through-the-thickness is direction 3), F_{1c} and F_{1t} are the compressive and tensile strengths along the in-plane direction, F_{3c} and F_{3t} are the compressive and tensile strengths along the through-the-thickness direction and $F_5(= F_{13})$ is the shear strength on the 1–3 plane.

The state of deformation and failure mechanisms in the core were studied by means of moire method. Figure 2 shows moire fringe patterns in the core of a sandwich beam with Divinycell H250 core under three-point bending. The moire fringe patterns corresponding to the horizontal and vertical displacements away from the applied load consist of nearly parallel and equidistant fringes from which it follows that the normal strains are zero, while the shear strain is nearly constant across the core thickness. This is valid only in the linear range.

Indentation failure. Indentation failure was observed in beams under three-point bending when no special reinforcement of the facing or the core was provided in the area under the load. Figure 3 shows the variation of the applied load with the displacement of the indenting roller for a 36 cm long beam under three-point bending. The displacement represents the sum of the global beam deflection and the local indentation, but it is more sensitive to the local indentation. Therefore, the proportional limit of the load-displacement curve is a good indication of initiation

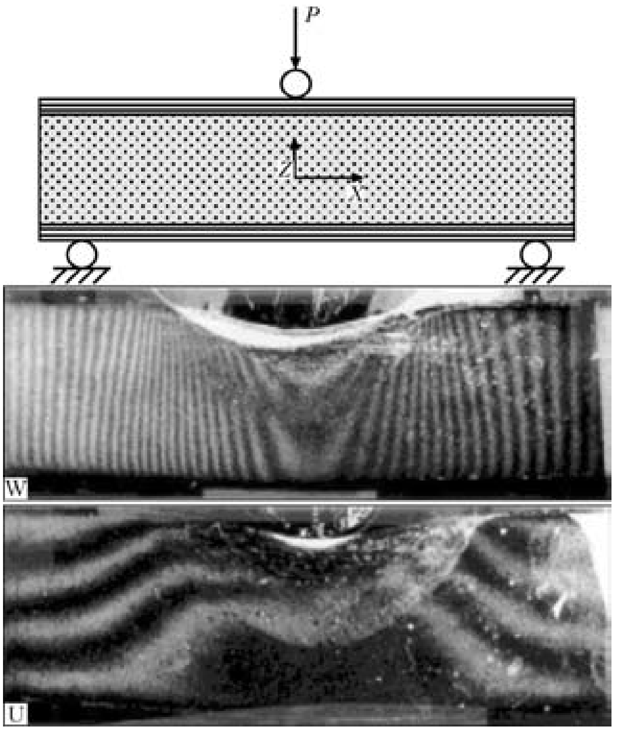

Figure 2. Moire fringe patterns corresponding to horizontal and vertical displacements in sandwich beam under three-point bending (12 lines/mm; Divinycell H250 core)

of indentation. In the present case the beam was made with a Divinycell H100 core. The load at initiation of indentation is 735 N. The peak load measured was P_{max} = 1080 N.

The indentation failure of the sandwich beam can be predicted by treating the loaded face as a beam resting on a foundation. For linear elastic behavior, the core is modeled as continuous distributed linear tension/compression springs. The stress σ at the interface between core and facing is proportional to the local deflection, w

$$\sigma = kw, \tag{5}$$

where k is the foundation modulus given by [10].

$$k = 0.64\,\frac{E_{c3}}{h_f}\,\sqrt[3]{\frac{E_{c3}}{E_{f1}}}. \tag{6}$$

For a long (assumed infinite) facing the deflection w_P under the load P is [10]

$$w_P = \frac{P\lambda}{2kb}, \tag{7}$$

where

$$\lambda = \frac{1.18}{h_f}\,\sqrt[3]{\frac{E_c}{E_{f1}}} \tag{8}$$

and b is the width of the facing.

Yield of the core under the load occurs when the interfacial stress σ reaches the yield stress of the foam core. The critical load at initiation of core yield is calculated from Eqs. (5) to (8) and the yield condition as

$$P_{cy} = 1.70\sigma_{ys}bh_f\,\sqrt[3]{\frac{E_{f1}}{E_c}}, \tag{9}$$

where σ_{ys} is the yield stress of the core.

As the load increases beyond the yield value, plastic deformation propagates through the core from the center to the ends of the facing. For a rigid-perfectly plastic foundation the local bending stress at the upper surface of the facing is given by [11]

$$\sigma_{ft} = \frac{9P^2}{16b^2h_f^2\sigma_{ys}}. \tag{10}$$

For a beam in three-point bending the global stress in the facing is

$$\sigma_{fb} = \frac{PL}{4bh_f(h_f + h_c)}, \tag{11}$$

where h_c is the thickness of the facing.

Indentation failure occurs when the sum of the local and global bending stresses, σ_{ft} and σ_{fb}, reaches the compressive strength of the facing

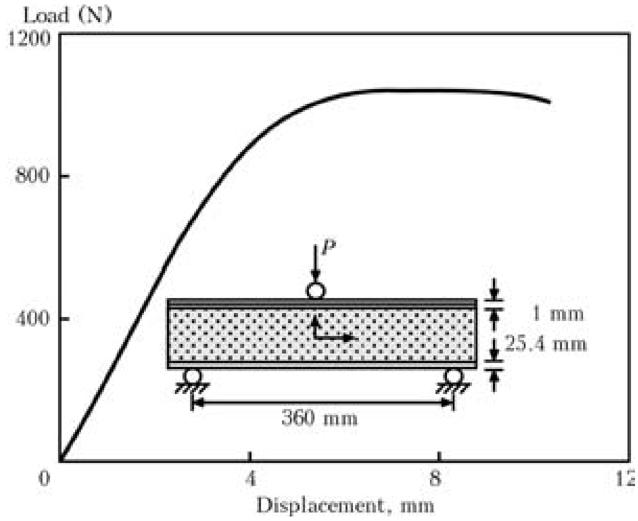

Figure 3. Load versus deflection under load of sandwich beam under three-point bending (carbon/epoxy facings, Divinycell H100 core)

material. The load at initiation of indentation in Figure 3 is 735 N and agrees with the calculated value of 800 N from Eq. (9). The peak load measured is P_{max} = 1080, while the calculated value is P_{max} = 1310 N. The difference in the results may be attributed in the simplifying assumption of a rigid-perfectly plastic foundation.

Failure mode transition. From the above discussion it is obvious that initiation of a particular failure mode depends on the geometrical characteristics, the material properties and the loading conditions of the beam. In the case of beams under three-point bending when reinforcement of the facings or the core is provided to suppress indentation failure, the prevalent failure modes are facing wrinkling and core failure. For short spans, core failure occurs first and then it triggers facing wrinkling. For long spans, facing wrinkling can occur before any core failure. Thus, a curve for the critical load for core failure initiation versus span length is obtained. On the other hand, the critical load for facing wrinkling as a function of span length can be predicted from Eq. (2). Figure 4 shows curves of the critical

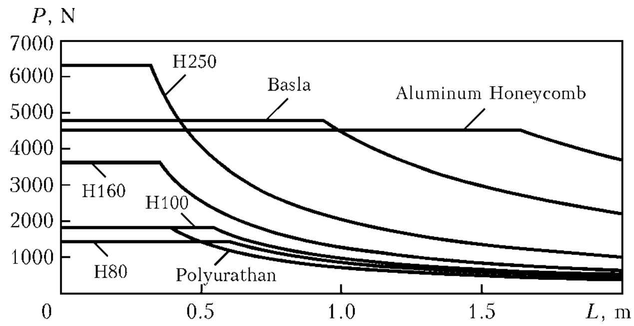

Figure 4. Critical load versus span length for failure initiation in sandwich beams under three-point bending. Horizontal lines indicate core shear failure and curved lines indicate failure by compressive facing wrinkling

load versus span length for initiation of failure by core failure and facing wrinkling for a sandwich beam with various core materials. The intersection of the curves defines the transition from core failure initiation to facing wrinkling initiation. Note that for core materials H250, balsa wood and aluminum honeycomb with increased through-the-thickness Young's modulus the compressive facing wrinkling failure curve is displaced, according to Eq. (2) to the right, and therefore, the critical length for failure mode transition from core failure to wrinkling increases. Thus, as the through-the-thickness Young's modulus of the foam increases, the critical length of the beam for failure mode transition from core failure to wrinkling, also increases.

Conclusions

Failure modes of composite sandwich beams depend on the type of loading, constituent material properties and geometrical dimensions. For sandwich beams made of unidirectional carbon/epoxy facings and PVC closed-cell foam cores failure modes observed and studied include core failure, compressive facing wrinkling and indentation failure. Experimental results were compared with theoretical predictions whenever they were available. Following initiation, interaction of failure modes takes place leading to catastrophic fracture. Thus, failure initiation by plastic deformation of the core degrades the supporting role of the core and precipitates other failure modes, such as facing wrinkling. When core failure and stiffness degradation occur first, the critical wrinkling stress is substantially reduced. Thus, catastrophic failure of a sandwich beam appears to be the result of initiation propagation and interaction of failure modes, as influenced by type of loading, constituent material properties and geometrical dimensions.

1. Daniel, I.M., Gdoutos, E.E., Wang, K.-A. et al. (2002) Failure modes of composite sandwich beams. *Int. J. Damage Mech*, **11**, 309–334.
2. Gdoutos, E.E., Daniel, I.M., Wang, K.-A. (2002) Indentation failure in composite sandwich structures. *Exp Mech*, **42**, 426–431.
3. Daniel, I.M., Gdoutos, E.E., Wang, K.-A. (2002) Failure of composite sandwich beams. *Adv. Com. Letters*, **11**, 49–57.
4. Abot, J.L., Daniel, I.M., Gdoutos, E.E. (2002) Contact law for composite sandwich beams. *Sandwich Struct. & Mater*. **4**, 157–173.
5. Gdoutos, E.E., Daniel, I.M., Wang, K.-A. (2003) Compression facing wrinkling of composite sandwich structures. *Mech. Mater*., **35**, 511–522.
6. Gdoutos, E.E., Daniel, I.M., Wang, K.-A. (2000) Failure of cellular foams under multiaxial loading. *Comps. Part A*, **33**, 163–176.
7. Heath, W.G. (1969) Sandwich construction. Pt 2: The optimum design of flat sandwich panels. *Aircraft Engng*, **32**, 230–235.
8. Hoff, N.J., Mautner, S.E. (1945) The buckling of sandwich-type panels. *J. Aerosp. Sci*., **12**, 285–297.
9. Tsai, S.W., Wu, E.M. (1971) A general theory of strength for anisotropic materials. *J. Comp. Mat*., **5**, 58–80.
10. Hetenyi, M. (1946) *Beams on Elastic Foundation*. The University of Michigan Press.
11. Soden, P.D. (1996) Indentation of composite sandwich beams. *J. Strain Anal*., **31**, 353–360.

Received 08.04.2013